Pergamon

SCIENCE DIRECT

Bioorganic & Medicinal Chemistry 11 (2003) 2519–2527

BIOORGANIC & MEDICINAL CHEMISTRY

N-[^{18}F]fluoroethyl-4-piperidyl Acetate ([^{18}F]FEtP4A): A PET Tracer for Imaging Brain Acetylcholinesterase In Vivo

Ming-Rong Zhang,[a,b,*] Kenji Furutsuka,[a,b] Jun Maeda,[a,b] Tatsuya Kikuchi,[a,c] Takayo Kida,[a,b] Takashi Okauchi,[a,b] Toshiaki Irie[a] and Kazutoshi Suzuki[a]

[a]*Department of Medical Imaging, National Institute of Radiological Sciences, 4-9-1 Anagawa, Inage-ku, Chiba 263-8555, Japan*
[b]*SHI Accelerator Service Co. Ltd., 5-9-11, Kitashinagawa, Shinagawa-ku, Tokyo 141-8686, Japan*
[c]*Department of Pharmaceutical Sciences, Chiba University, 1-1-1 Yayoi, Inage-ku, Chiba 263-8522, Japan*

Received 14 January 2003; accepted 11 March 2003

Abstract—*N*-[^{18}F]Fluoroethyl-4-piperidyl acetate ([^{18}F]FEtP4A) was synthesized and evaluated as a PET tracer for imaging brain acetylcholinesterase (AchE) in vivo. [^{18}F]FEtP4A was previously prepared by reacting 4-piperidyl acetate (P4A) with 2-[^{18}F]fluoroethyl bromide ([^{18}F]FEtBr) at 130 °C for 30 min in 37% radiochemical yield using an automated synthetic system. In this work, [^{18}F]FEtP4A was synthesized by reacting P4A with 2-[^{18}F]fluoroethyl iodide ([^{18}F]FEtI) or 2-[^{18}F]fluoroethyl triflate ([^{18}F]FEtOTf in improved radiochemical yields, compared with [^{18}F]FEtBr under the corresponding condition. Ex vivo autoradiogram of rat brain and PET summation image of monkey brain after iv injection of [^{18}F]FEtP4A displayed a high radioactivity in the striatum, a region with the highest AchE activity in the brain. Moreover, the distribution pattern of ^{18}F radioactivity was consistent with that of AchE in the brain: striatum > frontal cortex > cerebellum. In the rat and monkey plasma, two radioactive metabolites were detected. However, their presence might not preclude the imaging studies for AchE in the brain, because they were too hydrophilic to pass the blood–brain barrier and to enter the brain. In the rat brain, only [^{18}F]fluoroethyl-4-piperidinol ([^{18}F]FEtP4OH) was detected at 30 min postinjection. The hydrolytic [^{18}F]FEtP4OH displayed a slow washout and a long retention in the monkey brain until the PET experiment (120 min). Although [^{18}F]FEtP4A is a potential PET tracer for imaging AchE in vivo, its lower hydrolytic rate and lower specificity for AchE than those of [^{11}C]MP4A may limit its usefulness for the quantitative measurement for AchE in the primate brain.

Introduction

Postmortem studies in patients with Alzheimer's disease (AD) suggested that, the most profound change, compared with normal subjects, is a progressive, inexorable reduction in the activity of acetylcholinesterase (AchE) in the neocortex and hippocampus.[1–4] Positron emission tomography (PET) has been used to measure the AchE activity and to offer the means for longitudinal study of AchE by imaging this enzyme in human brains with normal aging and in different stages of AD.[5–10] Using acetylcholine as a lead compound, a series of positron emitter-labeled acetylcholine analogues have been synthesized and evaluated for this purpose.[11–13] Of these radiotracers, *N*-[^{11}C]methyl-4-piperidyl acetate ([^{11}C]MP4A, Scheme 1) was a successful PET tracer for measuring the AchE activity and elucidating the relation between AchE and AD in the human brains.[14–16] [^{11}C]MP4A provided an index of regional AchE activity and kinetic modeling techniques as shown in Scheme 1.[14–16] After injecting this tracer into a subject, [^{11}C]MP4A penetrated across the blood–brain barrier (BBB) and was then metabolized by AchE to *N*-[^{11}C]methyl-4-piperidinol ([^{11}C]MP4OH), which resulted in a long-term retention of radioactivity in the brain.

In PET chemistry, ^{18}F-labeled radiotracers have several advantages over ^{11}C-labeled tracers. Due to the longer half-life of ^{18}F (β^+; 96.7%, $t_{1/2} = 109.8$ min), ^{18}F is convenient for long-time storage and long-distance transportation, and multiple doses can be prepared in one synthetic run. Moreover, due to the shorter positron range of ^{18}F than that of ^{11}C (650 KeV vs 960 KeV), ^{18}F often gives a slightly higher quality image with higher spatial resolution. Since PET measurement for AchE activity often requires over 40 min, a ^{18}F-

*Corresponding author. Tel.: +81-43-206-4041; fax: +81-43-206-3261; e-mail: zhang@nirs.go.jp

0968-0896/03/$ - see front matter © 2003 Elsevier Science Ltd. All rights reserved.
doi:10.1016/S0968-0896(03)00177-9

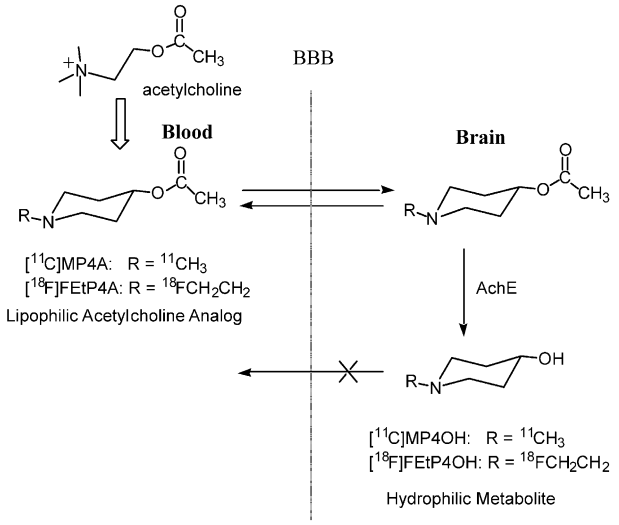

Scheme 1. Schematic diagram representing the biochemical rational of the radioactive acetylcholine analogue method for mapping AchE activity in the brain in vivo.

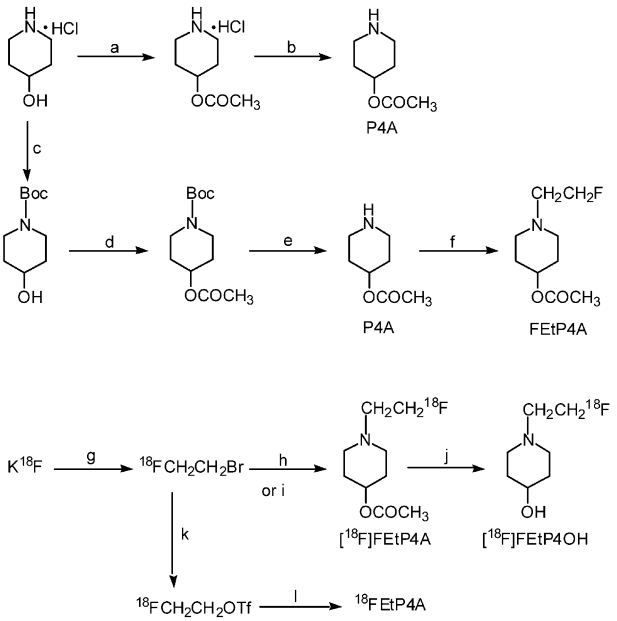

Scheme 2. Chemical synthesis and radiosynthesis: (a) CH_3COCl, 25 °C, 18 h; (b) 10% NH_3/H_2O, 0 °C, 5 min; (c) $(t\text{-Boc})_2O$, NaOH, 25 °C, 1 h; (d) $(CH_3CO)_2O$, pyridine, 25 °C, 6 h; (e) CF_3COOH, 0 °C, 1 h; (f) FCH_2CH_2Br, $i\text{-Pr}_2NEt$, NaI, 70 °C, 5 h; (g) $TfOCH_2CH_2Br$, 130 °C, 5 min; (h) P4A, 130 °C, 30 min; (i) P4A, NaI, 130 °C, 10 min; (j) NaOH, 95 °C, 5 min; (k) AgOTf, 300 °C, 10 min; (l) P4A, 25 °C, 10 min, 25 °C.

labeled tracer may be favorable over a ^{11}C-labeled tracer to gain more precise information about AchE activity. Based on this consideration, using [^{11}C]MP4A as a lead compound, we synthesized *N*-[^{18}F]fluoroethyl-4-piperidyl acetate ([^{18}F]FEtP4A, Scheme 1) as a putative tracer for AchE.[17] First, comparing acetylcholine and MP4A, FEtP4A with the *N*-fluoroethyl group was more lipophilic and could readily enter the brain, which is a prerequisite for a suitable PET tracer. Second, in the development of acetylcholine analogues, it was found that two methyl or ethyl groups were essential for acceptance by AchE, but the third methyl group could be replaceable with a longer alkyl chain.[18–20] Therefore, introducing the fluoroethyl group for the methyl group into the piperidine ring might not change its specificity for AchE. Third, *N*-[^{18}F]fluoroethyl-4-piperidinol ([^{18}F]FEtP4OH), a hydrophilic metabolite resulting from the specific hydrolysis of [^{18}F]FEtP4A by AchE, may be trapped and retained at the sites of AchE in the brain (Scheme 1).

In a previous study, we reported the radiosynthesis and distribution of [^{18}F]FEtP4A in the mouse brain.[17] [^{18}F]FEtP4A was synthesized by reacting piperidyl 4-acetate (P4A) with 2-[^{18}F]fluoroethyl bromide ([^{18}F]FEtBr) at 130 °C for 30 min with a 37% radiochemical yield (corrected for decay, based on the total [^{18}F]FEtBr) (Scheme 2). Due to its high uptake into the brain and distribution pattern corresponding to AchE in the mouse brain, [^{18}F]FEtP4A appeared to be ideally suited for PET imaging of AchE. However, the relatively low radiochemical yield and long synthetic time for [^{18}F]FEtP4A precluded further evaluation which required a large amount of this tracer. Therefore, we attempted to increase the fluoroethylation efficiency of P4A for producing [^{18}F]FEtP4A in a higher radiochemical yield, and then to evaluate this tracer by imaging AchE in rat and monkey brains in vivo and characterizing its enzymatic property.

We herein report (1) radiosynthesis of [^{18}F]FEtP4A by the respective fluoroethylation of P4A with [^{18}F]FEtBr, [^{18}F]FEtBr/NaI and 2-[^{18}F]fluoroethyl triflate[21,22] ([^{18}F]FEtOTf); (2) imaging study for AchE in the rat brain using ex vivo autoradiography and in the monkey brain using PET; (3) analysis for metabolites of [^{18}F]FEtP4A in plasma and the brain of rats, and plasma of monkey; (4) characterization of enzymatic property in vitro.

Results and Discussion

Chemistry

4-Piperidinol acetate (P4A), the substrate for radiosynthesis, was previously prepared by the acetylation of 4-piperidinol hydrochloride (Scheme 2).[17] However, the selective *O*-acetylation required a long time (18–25 h) at 25 °C, because no base could be used for this reaction where the *N*-acetylation occurred readily. Under this limited condition, 4-piperidinol hydrochloride reacted with acetyl chloride to give P4A only at a low yield of 12%. Recently, an improved chemical synthesis for P4A was carried out by protecting the *N* atom in the piperidine ring with *t*-butoxycarbonyl (Boc) group, and then reacting with acetic anhydride in the presence of pyridine. After the *O*-acetylation finished perfectly, the Boc group was removed with trifluoroacetic acid to give P4A at a total yield of 71% starting from 4-piperidinol hydrochloride (Scheme 2). This route provided a convenient and reliable method for preparing P4A.

We developed an automated system for synthesizing ^{18}F-labeled compounds using [^{18}F]FEtBr as a synthetic precursor.[17,23,24] Using this system, we prepared [^{18}F]FEtBr by heating [^{18}F]F^- with 2-bromoethyl triflate

($BrCH_2CH_2OTf$) in a reproducible radiochemical yield of 60–75% (corrected for the decay, based on total $[^{18}F]F^-$), and synthesized several [^{18}F]fluoroethylated ligands including [^{18}F]FEtP4A.[23,24] However, the lower reactivity of [^{18}F]FEtBr with substrates containing amine, phenol and other nucleophilic functional groups than that of $[^{11}C]CH_3I$ limited its wide application as a fluoroalkylating agent. P4A reacted rapidly with $[^{11}C]CH_3I$ at 70 °C for 3 min to give [^{11}C]MP4A with a high radiochemical yield of 60–85%. In contrast to [^{11}C]MP4A, P4A reacted with [^{18}F]FEtBr to afford [^{18}F]FEtP4A only at a poor yield of $<5\%$ under the same condition. In this time, to increase the reactivity of [^{18}F]FEtBr with P4A and to augment the radiochemical yield of [^{18}F]FEtP4A, [^{18}F]FEtBr was converted into more reactive (1) [^{18}F]FEtI in situ by adding tiny amounts of NaI to the fluoroethylation reaction mixture in advance; (2) [^{18}F]FEtOTf[21] by transferring [^{18}F]FEtBr into a heated column[22] containing sliver triflate (Scheme 2).

Table 1 shows the radiochemical yields and synthetic results of [^{18}F]FEtP4A under various reaction conditions. The reaction efficiency of P4A with [^{18}F]FEtBr/NaI or [^{18}F]FEtOTf was significantly augmented, compared with [^{18}F]FEtBr. When NaI (1 mg) was added to the reaction mixture in advance, P4A reacted with [^{18}F]FEtBr/NaI at 130 °C for 10 min to give [^{18}F]FEtP4A at a 74% radiochemical yield, whereas, without NaI, the reaction of P4A with [^{18}F]FEtBr afforded [^{18}F]FEtP4A only at an 18% yield under the same conditions. On the other hand, [^{18}F]FEtOTf displayed a higher reactivity with P4A than [^{18}F]FEtBr as well as [^{18}F]FEtBr/NaI. [^{18}F]FEtOTf was synthesized by flowing [^{18}F]FEtBr into a heated (300 °C) column containing silver triflate (AgOTf) with helium gas (30–50 mL/min). After trapping [^{18}F]FEtOTf into the reaction mixture for 10 min at 25 °C, 71% of the total radioactivity was found to represent [^{18}F]FEtP4A, and 29% was [^{18}F]FEtBr (Table 1). Since P4A did not react with [^{18}F]FEtBr at 25 °C, the conversion efficiency of [^{18}F]FEtBr into [^{18}F]FEtOTf was at least 71%.

After the [^{18}F]fluoroethylation reaction was terminated, the radioactive mixture was purified using a reverse semi-preparative HPLC system. It was of paramount importance in the synthesis of [^{18}F]FEtP4A to remove all traces of the unreacted substrate P4A, because P4A might have a certain specificity to AchE and obscure the imaging studies. Complete separation of [^{18}F]FEtP4A ($t_R = 9.8$–11.2 min) from P4A ($t_R = 5.2$–7.5 min) could be accomplished under the present conditions as shown in the experimental. Using radio-TLC, the identity for [^{18}F]FEtP4A was confirmed by the observation of co-elution with authentic non-radioactive FEtP4A. The radiochemical purity of [^{18}F]FEtP4A was determined to be $97.2 \pm 1.8\%$ for all formulations with an analytical reverse HPLC system. Since FEtP4A displays no special absorption on UV spectrum (200–400 nm), the specific activity of [^{18}F]FEtP4A at the end of synthesis was estimated to be 70–110 GBq/μmol from that of [^{18}F]FEtBr prepared in other synthetic runs. In the final product solution (10 mL), the contamination of P4A was quantified by LC/MS to be 0.6–1.4 μg, which met the specification of a radiopharmaceutical product provided for clinical use in our facility. The stability of [^{18}F]FEtP4A in its prepared form was evaluated by monitoring its radiochemical purity using the same analytic HPLC. The radiochemical purity remained $>95\%$ after maintenance of the [^{18}F]FEtP4A preparation at 25 °C for 4 h at the radioactivity concentration of 37–65 MBq/mL. On the other hand, *N*-[^{18}F]fluoroethyl-4-piperidinol ([^{18}F]FEtP4OH), a possible radioactive metabolite of [^{18}F]FEtP4A, was prepared by hydrolyzing the parent compound with 0.1 N NaOH at $>98\%$ radiochemical yield (Scheme 2).

Evaluation

Using [^{11}C]MP4A as a lead compound, we synthesized [^{18}F]FEtP4A as a putative PET imaging agent for AchE in vivo.[17] On the basis of structural similarity, it was anticipated that [^{18}F]FEtP4A would mimic the distribution and metabolism of [^{11}C]MP4A, resulting in a similar acceptance by AchE. The preliminary study on mice displayed that the initial uptake of [^{18}F]FEtP4A into the mouse brain reached 8% injected dose/g tissue, and its radioactivity distribution was consistent with the distribution pattern of AchE activity in the brain: striatum > cerebral cortex > cerebellum.[17] Moreover,

Table 1. Radiosynthesis results of [^{18}F]FEtP4A under various conditions

Reagent	Reaction temperature (°C)	Reaction time (min)	Radiochemical yield[a] (%)	Purification yield[b] (%)	Synthesis time[c] (min)
	25	10	No reaction		
	70	10	8		
$[^{18}F]FCH_2CH_2Br$	130	10	18		
	130	20	32		
	130	30	56	39	78
	25	10	3		
	70	10	29		
$[^{18}F]FCH_2CH_2Br$/NaI	130	10	74	64	59
	130	20	86		
	130	30	90		
	25	10	71	50	48
$[^{18}F]FEtOT_f$	70	10	67		

[a]Radiochemical yield as determined by analytic HPLC from a sample withdrawn from the reaction mixture.
[b]Decay corrected radiochemical yield (%) after HPLC purification based on the total [^{18}F]FEtBr.
[c]From EOB, including the recovery of $[^{18}F]F^-$ from the target.

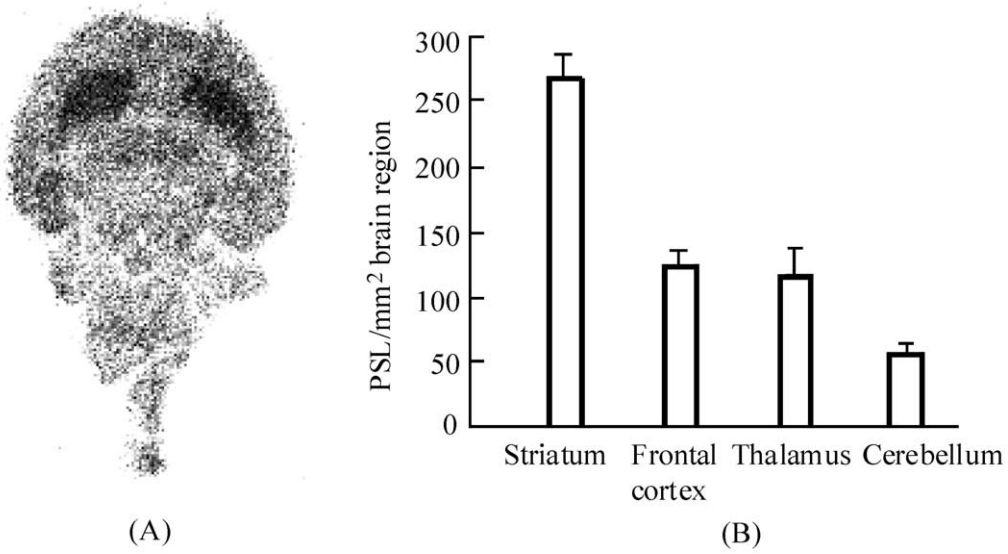

Figure 1. A: Ex vivo autoradiogram of [^{18}F]FEtP4A in the striatal section of the rat brain at 30 min postinjection (20 MBq). B: Ex vivo autoradiographic localizations of ^{18}F radioactivity in the sagittal sections of rat brains ($n=3$) at 30 min postinjection of [^{18}F]FEtP4A. The regional uptake of ^{18}F was expressed as photo-stimulated-luminescence (PSL) values per square millimeter of brain section (PSL/mm^2).

[^{18}F]FEtP4A was rapidly hydrolyzed to [^{18}F]FEtP4OH in the mouse brain after injection.[17] Thus, [^{18}F]FEtP4A appeared to be a promising PET tracer for AchE in vivo. These results prompted us to evaluate the tracer in rats and monkey by imaging AchE using ex vivo autoradiography and PET, and characterizing its enzymatic property.

Figure 1 shows the autoradiographic localizations of ^{18}F-radioactivity in the rat brain at 30 min postinjection of [^{18}F]FEtP4A. As can be seen in the sagittal section, a significant radioactivity was observed in the striatum (Fig. 1a,b), while a modest uptake was present in the frontal cortex and thalamus, and the lowest uptake was in the cerebellum (Fig. 1b). The radioactivity in the striatum was approximately 3-fold or 2-fold higher than that in the frontal cortex and thalamus or cerebellum (Fig. 1b).

Figure 2 shows a PET image of the monkey brain acquired from 0 to 120 min after [^{18}F]FEtP4A injection (88 MBq/1.5 mL). This image displays evident accumulation of radioactivity in the striatum compared with the other regions (frontal cortex, thalamus and cerebellum), which was similar with the autoradiogram of the rat brain.

Figure 3 shows time–activity curves (TACs) of [^{18}F]FEtP4A in the striatum, frontal cortex, thalamus and cerebellum after injection of [^{18}F]FEtP4A (88 MBq) into the monkey. Immediately following iv administration, the radioactivity began to accumulate in the brain regions. The initial uptake of [^{18}F]FEtP4A into the monkey brain was high, reflecting a high penetration of the tracer across the monkey BBB consistent with its partition coefficient of 0.78,[17] which is favorable for the permeability of the tracer across the BBB. The radioactivity in all regions examined reached a peak by 3–5 min postinjection, and then showed a rapid washout from all structures until 10 min. At 10 min postinjection, the ^{18}F radioactivity in the striatum was greater than 2-fold those in the frontal cortex, thalamus and cerebellum. From then, a slow decline of radioactivity was seen from the striatum, from which the concentration of ^{18}F at the end of the PET scan (120 min) was reduced to half the 10-min value. On the other hand, the radioactivities in the frontal cortex, thalamus and cerebellum remained on plateau levels until the end of PET scan.

In imaging studies of the brain, the presence of metabolites in the plasmas of experimental animal might preclude the evaluation of a PET tracer if the metabolites entered the brains and were retained/bound at the

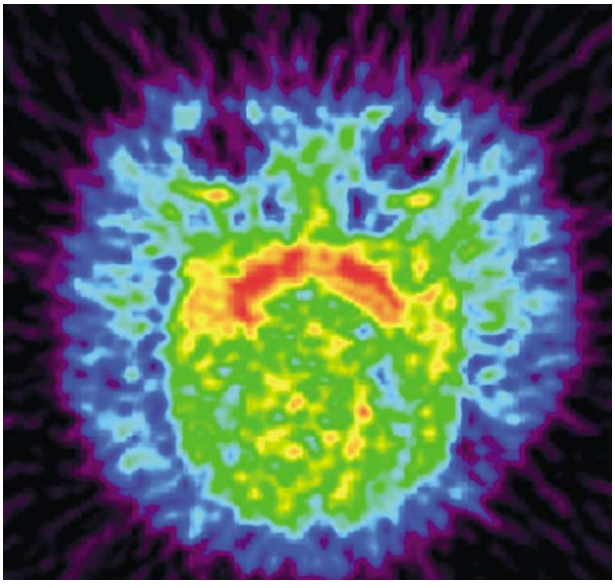

Figure 2. PET summation image of midstriatial/midthalamic level of the monkey brain acquired between 0 and 120 min after [^{18}]FEtP4A injection (88 MBq).

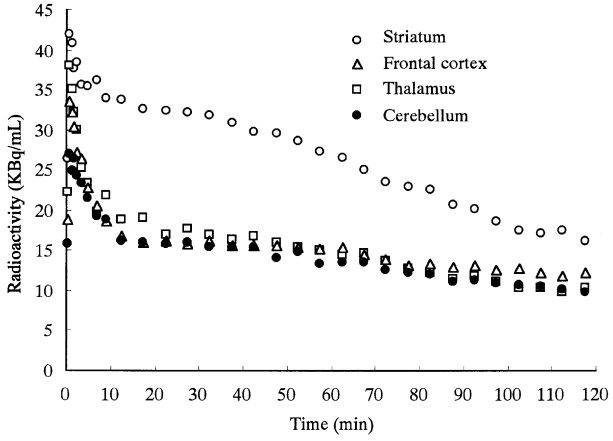

Figure 3. Time–activity curves (TACs) in the striatum, thalamus, frontal cortex and cerebellum of the monkey brain after iv injection of [^{18}F]FEtP4A (88 MBq).

target sites. Therefore, it is necessary to determine whether the radioactive metabolites in the brain were contributing to the signal observed in vivo. Chemical analyses of the radioactive metabolite(s) of [^{18}F]FEtP4A in the plasma and brain were carried out using radio-TLC and HPLC. After iv administration of [^{18}F]FEtP4A (20 MBq) into rats ($n=3$) at 30 min, the plasma and brain homogenate were respectively obtained and immediately deproteinized with CH_3CN. Extraction[25] of the radioactivity in the plasma in addition to the brain into CH_3CN proved to be efficient (>70%). In the HPLC analysis for plasma samples, three radioactive components were observed. Using radio-TLC, two of these fractions were respectively identified to be unchanged [^{18}F]FEtP4A (2% of total radioactivity) and the hydrolysate [^{18}F]FEtP4OH (77%). In addition to the two fractions, an unknown product (21%) that was too polar to be retained on the column under the present conditions was also detected. By treating this product with 10% Na_2CO_3 solution, it was entirely changed to [^{18}F]FEtP4OH, suggesting it was glucuronidated [^{18}F]FEtP4OH, the most common product of phase II metabolism.[26] On the other hand, only [^{18}F]FEtP4OH was detected in the homogenate sample of rat brains at 30 min postinjection.

After iv injection of [^{18}F]FEtP4A into the monkey, [^{18}F]FEtP4A in the monkey plasma decreased rapidly from 100 to 45% at 10 min (Fig. 4). From then, the amount of unchanged [^{18}F]FEtP4A continued to decrease, while those of [^{18}F]FEtP4OH and the same product determined in the rat plasma increased slowly during the entire PET experiment. The fraction corresponding to [^{18}F]FEtP4A in the plasma was 25% at 20 min, 17% at 30 min, and 16% at 60 min of the total radioactivity. At the end of the PET scan (120 min), [^{18}F]FEtP4A was entirely transformed to [^{18}F]FEtP4OH and the putative glucuronidated [^{18}F]FEtP4OH. Since [^{18}F]FEtP4OH (partition coefficient: 0.06)[17] in addition to the water-soluble product displayed high hydrophilicities, they could not cross the BBB and enter the brain. The very low uptake (<0.6% dose/g) of [^{18}F]FEtP4OH into the mouse brain was also determined in the mouse brain.[17] These findings suggested

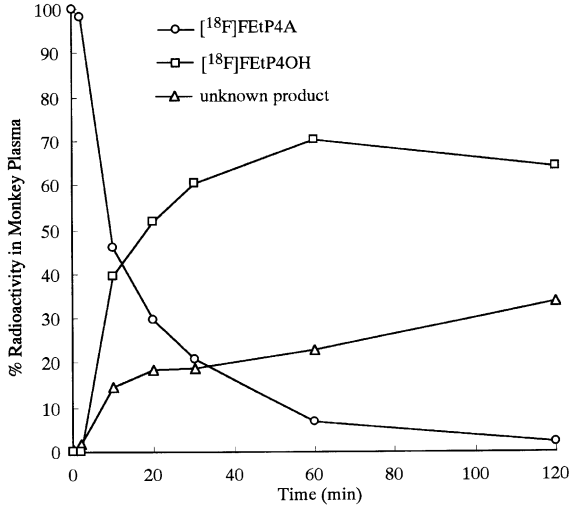

Figure 4. Percent conversion of [^{18}F]FEtP4A to metabolites in plasma at several time points after iv injection of [^{18}F]FEtP4A (50 MBq) into the monkey. The metabolites and unchanged [^{18}F]FEtP4A were analyzed by HPLC for CH_3CN extracts from plasma and brain prepared as described in the experimental.

that the exchange of two metabolites between the blood and brain was small in the rat and monkey, although [^{18}F]FEtP4A was extensively metabolized in the plasma. Thus, the presence of metabolites in the blood did not obscure the signals acquired from the ex vivo autoradiogram of the rat brain and PET image of the monkey brain.

Since (1) the ^{18}F radioactivity of showed a slow washout from the monkey brain and displayed a relatively long-term retention in the brain as shown in the TAC of [^{18}F]FEtPA for the monkey; (2) only [^{18}F]FEtP4OH was detected in the rat homogenates, the autoradiogram and PET images obtained in these studies reflected the distribution of AchE in the brains. However, whether [^{18}F]FEtP4A could be used for the quantitative measurement of AchE activity in a primate brain depends upon its specificity for AchE and the hydrolytic rate by AchE in the brain. Therefore, the enzymatic hydrolysis rate and specificity to AchE of [^{18}F]FEtP4A were measured and compared with [^{11}C]MP4A using rat brain homogenates. The hydrolysis rates and specificity measurements of [^{18}F]FEtP4A and [^{11}C]MP4A are shown in Table 2. [^{18}F]FEtP4A displayed a 14-fold slower rate of hydrolysis in the rat brain homogenate in vitro than [^{11}C]MP4A. The specificity of [^{18}F]FEtP4A for AchE was reduced to 71%, compared with that (96%) of [^{11}C]MP4A. The reason of the differences between the enzymatic hydrolysis rates and specificities of two tracers were due to the discrepancy of *N*-methyl and *N*-fluoroethyl groups. Introduction of the bulky and electronegative fluoroethyl group into the piperidyl acetate molecule decreased the binding efficiency to the AchE, compared with the methyl group. Since the approach for measuring AchE activity in vivo demands complete hydrolysis of used PET tracer by this enzyme within designated scan times, the slower hydrolytic rate of [^{18}F]FEtP4A limited its usefulness for the quantitative determination for AchE in the primate brain. Moreover, the relatively low specificity of [^{18}F]FEtP4A

Table 2. Enzymatic hydrolysis rate and% AchE specificity of [^{18}F]FEtP4A and [^{11}C]MP4A in rat brain homogenate

	Hydrolysis rate[a] (min/g/mL)	Specificity for AchE[b] (%)
[^{18}F]FEtP4A	1.345	95.8
[^{11}C]MP4A	0.094	71.3

[a]First-order hydrolysis rate constant (fraction/min) for rat brain homogenate concentration of 1 g/mL, $n = 3$).
[b]BW284c51 (30 μM) was used as an inhibitor of AchE.

for AchE may reduce the accuracy of data if this tracer was used to measure quantitatively the AchE activity in the brain.

Conclusion

[^{18}F]FEtP4A was synthesized by the respective reaction of P4A with [^{18}F]FEtBr, [^{18}F]FEtBr/NaI and [^{18}F]FEtOTf. The order of the [^{18}F]fluoroethylation efficiency was [^{18}F]FEtOTf > [^{18}F]FEtBr/NaI > [^{18}F]FEtBr. The ex vivo autoradiography and PET imaging study demonstrated that [^{18}F]FEtP4A was a potential PET tracer for AchE in the rat and monkey. However, the lower hydrolytic rate and lower specificity for AchE of [^{18}F]FEtP4A may limit its usefulness for the quantitative measurement for AchE in the primate brain.

Experimental

General

^{1}H NMR spectra were recorded on a JNM-GX-270 spectrometer (JEOL, Tokyo) with tetramethylsilane as an internal standard. All chemical shifts (δ) were reported in parts per million (ppm) downfield from the standard. FAB-MS was obtained on a JEOL NMS-SX102 spectrometer (JEOL, Tokyo). Column chromatography was performed using Merck Kieselgel gel 60 F_{254} (70–230 mesh). 18-Fluorine (^{18}F) was produced by the ^{18}O (p, n) ^{18}F nuclear reaction using a CYPRIS HM-18 cyclotron (Sumitomo Heavy Industry, Tokyo). If not otherwise stated, radioactivity was determined with an IGC-3R Curiemeter (Aloka, Tokyo). HPLC was performed using a JASCO HPLC system (JASCO, Tokyo): effluent radioactivity was monitored using a NaI (Tl) scintillation detector system. All chemical reagents with the highest grade commercially available were purchased from Aldrich Chem. (Milwaukee, WI) and Wako Pure Chem. Ind. (Osaka). The animal experiments were carried out according to the recommendations of the committee for the care and use of laboratory animals, National Institute of Radiological Sciences (NIRS).

4-Piperidyl acetate (P4A). 4-Hydroxypiperidine hydrochloride (1.0 g, 7.3 mmol) was dissolved in distilled water (2 mL). To this solution was added 0.5 N NaOH solution (5 mL) and then di-*t*-butyl dicarbonate (1.8 g, 8.2 mmol) was added dropwise with vigorous stirring at 25 °C for 1 h. After quenching $CHCl_3$ with this mixture, the organic layer was washed with water, 27% ammonia water and saturated NaCl solution. After drying the organic layer with Na_2SO_4, the solvent was removed to afford a yellowish oil.

This oil was dissolved in a solution of pyridine (3 mL) and acetic anhydride (1 mL, 10.6 mmol), and the reaction mixture was stirred at 25 °C for 6 h. After quenching the reaction mixture with AcOEt, the organic layer was washed with water, 27% ammonia water and saturated NaCl solution. Drying the AcOEt layer over Na_2SO_4, and removing the solvent gave a colorless reactant. The reactant dissolved in CH_2Cl_2 (20 mL) was treated with trifluoroacetic acid (1.5 mL) at 0 °C, continuously stirred for 1 h at 0 °C and evaporated to dryness. The residue was dissolved in 1% ammonia water and extracted with CH_2Cl_2. After drying the organic layer with Na_2SO_4, the solvent was removed to give a crude oil. Column chromatograph of the crude product on silica gel and elution with $CHCl_3$/MeOH/27% ammonia water (9/1/0.01) provided P4A (590 mg, 57%) as a slightly yellowish crystal. ^{1}H NMR ($CDCl_3$) δ: 4.71–4.76 (1H, m), 2.27–2.51 (4H, m), 1.98 (3H, s), 1.58–1.88 (4H, m). IR (Nujol): 1720 cm^{-1}. FAB-MS (*m*/*z*) calcd for $C_9H_{16}FNO_2$ ($M^+ + 1$): 144; found: 144.

***N*-Fluoroethyl-4-piperidyl acetate (FEtP4A).** A mixture of P4A (1.0 g, 7.0 mmol), 1-bromo-2-fluoroethane (1.1 mL, 14.8 mmol), NaI (2.2 g, 14.7 mmol) and *i*-Pr_2NEt (1.5 mL, 17.2 mmol) in DMF (12.0 mL) was heated at 70 °C for 5 h. After cooling the reaction mixture, the mixture was quenched with AcOEt and washed with water, and saturated NaCl solution. After the organic layer was dried over Na_2SO_4, the solvent was removed to give a residue. Column chromatography of the residue on silica gel with $CHCl_3$ gave FEtP4A (990 mg, 74.8%) as a colorless oil. ^{1}H NMR ($CDCl_3$) δ: 4.71 (1H, m), 4.49 (2H, dt, $J_{H,F} = 40.1$ Hz, $J_{H,H} = 4.8$ Hz), 2.70 (2H, m), 2.58 (2H, dt, $J_{H,F} = 27.6$ Hz, $J_{H,H} = 4.8$ Hz), 2.28 (2H, m), 1.98 (3H, s), 1.58–1.88 (4H, m). IR (neat): 1730 cm^{-1}. FAB-MS (*m*/*z*) calcd for $C_9H_{16}FNO_2(M^+ + 1)$: 190; found: 190. Anal. calcd for $C_9H_{16}FNO_2$: C 57.14, H, 8.47, N 7.41; found: C 57.31, H 8.40, N 7.53.

***N*-[^{18}F]Fluoroethyl-4-piperidinyl acetate([^{18}F]FEtP4A).**

(1) Production of [^{18}F]F$^-$. [^{18}F]F$^-$ was produced by the ^{18}O (p,n) ^{18}F reaction on 10–20 atom% $H_2^{18}O$ using 18 MeV protons (14.2 MeV on target) from the cyclotron and separated from [^{18}O]H_2O using Dowex 1-X8 anion exchange resin in an irradiating room. The [^{18}F]F$^-$ was eluted from the resin with aqueous potassium carbonate (3.3 mg/0.3 mL) into a glass vial containing CH_3CN (1.5 mL)/Kryptofix 2.2.2. (25 mg) and transferred into a reaction vessel in a hot cell.

(2) Radiosynthesis of [^{18}F]FEtP4A via [^{18}F]FEtBr. After the [^{18}F]F$^-$ was dried to remove H_2O and CH_3CN from the reaction vessel, 2-bromoethyl triflate[31] ($BrCH_2CH_2OTf$) (8 μL) in *o*-dichlorobenzene (500 μL) was added into the radioactive solution. Then, the

[^{18}F]FEtBr that resulted in this vessel was distilled under a helium flow (90–100 mL/min) at 130 °C for 2 min and bubbled into another vessel containing a solution of anhydrous DMF (300 μL) and P4A (0.8 mg) at −20 °C. After maximum radioactivity was reached into the solution, the reaction mixture was warmed to 130 °C and maintained for 30 min. The content was diluted with an HPLC mobile phase (500 μL) and applied onto a semi-preparative column (10 mm ID×250 mm, Megapak SIL C18) attached to the JASCO HPLC system. Elution with 5 mM CH_3COONH_4 (pH = 4.9)/CH_3CN (9/1) at a flow rate of 4 mL/min gave a radioactive fraction corresponding to pure [^{18}F]FEtP4A (t_R = 9.8–11.2 min). The fraction was collected in a rotary evaporator and evaporated to dryness at 90 °C under reduced pressure. The residue was re-dissolved in 10 mL of saline and passed through a Millipore filter (GS, 0.22 μm) to provide an injectable solution of [^{18}F]FEtP4A for animal experiments. All the above procedures were carried out automatically by the use of a newly developed system.[23,24] Total synthesis time was 73 ± 5 min (n = 6) from the end of bombardment. At the end of the synthesis, 210 ± 90 MBq (n = 6) of [^{18}F]FEtP4A were obtained after 10–15 min proton bombardment at a beam current of 15 μA.

(3) Radiosynthesis of [^{18}F]FEtP4A via [^{18}F]FEtBr/NaI. The [^{18}F]FEtBr was trapped into a solution of anhydrous DMF (300 μL), NaI (1 mg) and P4A (0.8 mg) at −20 °C. After the reaction was finished, the radioactive mixture was treated as described above.

(4) Radiosynthesis of [^{18}F]FEtP4A via [^{18}F]FetOTf. The [^{18}F]FEtBr was passed through a heated steel column (3 mm ID×40 mm, oven temperature: 300 °C) containing AgOTf (100 mg) impregnated graphite carbon (300 mg) under helium gas flow (50 mL/min).[21,22] After trapping [^{18}F]FEtOTf into a solution of anhydrous DMF (300 μL) and P4A (0.8 mg) at 25 °C for 10 min, the reaction mixture was treated as described above.

***N*-[^{18}F]Fluoroethyl-4-piperidinol ([^{18}F]FEtP4OH).** A mixture of [^{18}F]FEtP4A (37 MBq) in 0.1 N aqueous NaOH solution (0.5 mL) was heated at 95 °C for 5 min. After adjusting the pH of the reaction solution to 6–7, the reaction solution containing [^{18}F]FEtP4OH with 96% radiochemical purity was used for identification and analysis of metabolites.

Identity confirmation. A solution of [^{18}F]FEtP4A or [^{18}F]FEtP4OH (2–3 μL) containing non-radioactive FEtP4A or FEtP4OH (1 mg/5 mL CH_3CN) was spotted on a silica gel TLC plate, which was then developed with $CHCl_3$/CH_3OH/27% ammonia water (4/1/0.01) as a mobile phase. The TLC plate was air-dried and placed in contact with a phosphor imaging plate (BAS-SR 127, Fujiphoto Film, Tokyo) for 10 min, and the radioactivity distribution on the plate was analyzed using a FUJI BAS 3000 bioimaging analyzer (Fujiphoto Film). [^{18}F]FEtP4A or [^{18}F]FEtP4OH was identified by comparing the Rf with the non-radioactive FEtP4A (R_f = 0.68) or FEtP4OH (R_f = 0.42) which was visualized by heating the TLC plate sprayed with ninhydrin solution.

Radiochemical purity determinations. Radiochemical purity of [^{18}F]FEtP4A or [^{18}F]FEtP4OH was assayed by analytical HPLC (column: Finepak Sil C18-10, JASCO, 4.6 mm ID × 250 mm). The mobile phase was 50 mM CH_3COONH_4 (pH = 3.1)/CH_3CN (3/7) for [^{18}F]FEtP4A and 50 mM CH_3COONH_4 (pH = 3.1)/CH_3CN (1/9) for [^{18}F]FEtP4OH, respectively. The t_R was 6.8 min for [^{18}F]FEtP4A and 5.6 min for [^{18}F]FEtP4OH at a flow rate of 2 mL/min, respectively.

Specific activity determination. Since FEtP4A displays no special absorption on a UV spectrum (200–400 nm), the specific activity of [^{18}F]FEtP4A was estimated from that of [^{18}F]FEtBr in the other synthetic run. The specific activity of [^{18}F]FEtBr was determined by comparison of UV absorbance of [^{18}F]FEtBr at 210 nm with those of known concentrations of FEtBr, which was obtained by HPLC analysis with CAPCELL PAK C_{18} column (4.6 mm ID × 250 mm). The t_R for [^{18}F]FEtBr was 4.5 min at a flow rate of 2.0 mL/min using a mobile phase of CH_3CN/H_2O (30/70).

Determination of P4A in the final product solution with LC-MS. After the radioactivity decayed, the final product solution of [^{18}F]FEtP4A (1 mL) was concentrated to 50 μL for analysis. The LC-MS system consisted of a Hewelett-Packard HPLC system (SERIES 1100, Hewelett-Packard Japan, Tokyo) and a Finepak Sil C18-10 column (10 μm, 4.6 mm ID × 250 mm; JASCO, Tokyo) eluted with 5 mM CH_3COONH_4 (pH = 4.9)/CH_3CN (8/2) at 0.75 mL/min. The effluent (5 μL) from the column was led into a Frit FAB ion source of the mass spectrometer (JEOL JMS-SX102A spectrometer; JEOL, Tokyo). The mass of P4A in the final solution was estimated by comparison of LC-MS detector response to m/z of P4A with the injected authentic standard.

Ex vivo autoradiography study in rat. Male ddy rats (n = 3) were sacrificed 30 min after iv injection of [^{18}F]FEtP4A (20 MBq). The brain tissue was removed and frozen in a freezer at −80 °C at 3 min, and the frozen tissue was cut into 20 μm thick horizontal sections. Each section was thawed on a cover glass, exposed to HCl vapor, dried on a hot plate for 10 s and placed in contact with a phosphor imaging plate (BAS-SR 127, Fujiphoto Film) for 60 min. The radioactivity distribution on the plate was analyzed using a FUJI BAS 3000 bioimaging analyzer (Fujiphoto Film). Regions of interest (ROIs) on the sections were placed on the striatum, thalamus, frontal cortex and cerebellum. The regional uptake of ^{18}F was expressed as photo-stimulated-luminescence (PSL) values per square millimeter of the brain section (PSL/mm^2).

PET study in monkey. PET scan was performed using a high-resolution SHR-7700 PET camera (Hamamatsu Photonics, Hamamatsu, Japan) designed for laboratory animals, which provides with 31 transaxial slices 3.6 mm (center-to-center) apart and a 33.1 cm field of view. A

male rhesus monkey (*macaca mulatta*) weighing about 5 kg was repeatedly anesthetized with ketamine (Ketalar®, 10 mg/kg/h, im) every h through the session. After transmission scans for attenuation correction were performed for 1 h using a 74 MBq ^{68}Ge-^{68}Ga source, a dynamic emission scan in 3-D acquisition mode was performed for 90 min (2 min × 5 scans, 4 min × 10 scans, 10 min × 4 scans). All emission scan images were reconstructed with a 4-mm Colsher filter, and circular regions of interest (ROIs) with a 5-mm diameter were placed over the striatum, frontal cortex, thalamus and cerebellum using image analysis software.[27] A solution of [^{18}F]FEtP4A (88 MBq) was injected iv into the monkey, and time-sequential tomographic scanning was performed on a transverse section of the brain for 120 min. The time–activity curves (TAC) in ROIs were obtained for each scan of the brain.

Metabolite analysis in rat plasma and brain homogenate. After iv administration of [^{18}F]FEtP4A (20 MBq/200 μL) into rats (ddy, $n=3$), these animals were sacrificed by cervical dislocation at 30 min postinjection. Blood (0.7–1.0 mL) and whole brains were respectively removed from these rats quickly. The blood sample was centrifuged at 15,000 rpm for 1 min at 4 °C to separate plasma, which (250 μL) was collected in a test tube containing CH_3CN (500 μL) and a solution of non-radioactive FEtP4A and FEtP4OH (10 μL, 0.5 mg/mL CH_3CN). After the tube was vortexed for 15 s and centrifuged at 15,000 rpm for 2 min, the CH_3CN supernatant was collected. The extraction efficiency of radioactivity into the supernatant ranged from 71 to 89% of the total radioactivity in the plasma. On the other hand, the cerebral cortex, striatum, thalamus and cerebellum were dissected from the rat brain and homogenized together in an ice-cooled $CH_3OH/CHCl_3$ (1/1; 1.5 mL) solution containing non-radioactive FEtP4A and FEtP4OH (0.5 mg/mL CH_3CN). The homogenate was centrifuged at 15,000 rpm for 1 min and the supernatant was collected. The recovery of radioactivity into the CH_3CN supernatant was 78–87% based on the total radioactivity in the brain homogenate.

An aliquot of the supernatant (100–500 μL) of plasma or brain homogenate was injected into the HPLC with a highly sensitive positron detector for radioactivity. The radioactivity in the fraction was analyzed using a Megapak SIL C18 column (10 mm ID × 250 mm) and an eluent of 5 mM CH_3COONH_4 (pH = 4.9)/CH_3CN 9/1 at a flow rate of 4 mL/min. The t_R for the unchanged [^{18}F]FEtP4A was 15.9 min, whereas that for [^{18}F]FEtP4OH or an unknown product was 6.2 or 1.8 min. The percent ratio of each radioactive fraction to the total radioactivity on the HPLC chromatogram was calculated as % = (peak area for the fraction /total peak area) ×100. Moreover, these fractions were respectively collected and identified using the radio-TLC described above: [^{18}F]FEtP4A, $R_f=0.68$; [^{18}F]FEtP4OH, $R_f=0.42$; the unknown product, $R_f<0.1$.

Metabolite analysis in monkey plasma. After iv injection of [^{18}F]FEtP4A (50 MBq) into the monkey, arterial blood samples (1 mL) were collected at periods of 2, 10, 30, 60, 90 and 120 min. All samples were centrifuged at 15,000 rpm for 1 min at 4 °C to separate plasma, which (250 μL) was collected in a test tube containing CH_3CN (0.5 mL). The tube was vortexed for 15 s and centrifuged at 15,000 rpm for 1 min for deproteinization. The extraction efficiency of radioactivity into the CH_3CN ranged from 78 to 94% of the total radioactivity in the plasma. The radioactive fractions in these plasma samples were determined using HPLC.

Characterization of enzymatic property using rat brain homogenate in vitro. Brain tissues from male ddy rats ($n=3$) were combined, weighed and homogenized in 0.1 M phosphate buffer (pH 7.4) with a glass-teflon homogenizer, and the homogenate was diluted to the final concentration of 35 mg/mL. Two hundreds μL of the homogenate and 100 μL of either the buffer alone or 1,5-bis(4-allydimethylammoniumphenyl)pentane-3-one dibromide (BW284c51, a specific inhibitor of AchE, 120 μM) solution were added to a reaction tube and preincubated for 5 min at 25 °C. The reaction was initiated by adding [^{18}F]FEtP4A (5 MBq) or [^{11}C]MP4A (20 MBq) in 100 μL of phosphate buffer. At designated time intervals, 200 μL of ethanol was added to each tube to stop the reaction. Three μL of the solution was then applied to a silical gel TLC plate. The TLC plates were developed and the radioactivities corresponding [^{18}F]FEtP4A, [^{11}C]MP4A and their metabolites in the TLC plates were determined according to the procedures as shown in the item of identity confirmation. The enzymatic hydrolysis rate of [^{18}F]FEtP4A or [^{11}C]MP4A was calculated as: $K = -\mathrm{Ln}(A_2/A_2)/(T_2 - T_1)/C$, where A_1 and A_2 represent the radioactivity of [^{18}F]FEtP4A or [^{11}C]MP4A at times T_1 and T_2, respectively, and C represents the concentration (g/mL) of the brain tissue in the reaction mixture. The AchE specificity of [^{18}F]FEtP4A or [^{11}C]MP4A in rat brain homogenate was calculate as: specificity $(\%) = 100 \times (K - K_1)/K$, where K_1 represents the rate constant in the brain homogenate added with BW284c51.

Acknowledgements

The authors thank the staff of the Cyclotron Section and Radiopharmaceuticals Section of the National Institute of Radiological Sciences (NIRS) for their support in the operation of the cyclotron and the production of radioisotopes.

References and Notes

1. Davis, P.; Maloney, A. *Lancet ii* **1976**, 1403.
2. Perry, E.; Perry, R.; Gary, B.; Bernard, E. *Lancet i* **1977**, 189.
3. Bierer, L.; Haroutunian, V.; Gabriel, S.; Knott, P.; Carlin, L.; Purohit, D.; Perl, D.; Schmeidler, J.; Kanof, P.; Davis, K. *J. Neurochem.* **1995**, *64*, 749.

4. Whitehouse, P.; Price, D.; Clark, A.; Coyle, J.; DeLong, M. *Ann. Neuro.* **1981**, *10*, 122.
5. Iyo, M.; Namba, H.; Fukushi, K.; Shinotoh, H.; Nakatsuka, S.; Suhara, T.; Sudo, Y.; Suzuki, K.; Irie, T. *Lancet* **1997**, *349*, 1805.
6. Kilbourn, M.; Sherman, P.; Snyder, S. *Nucl. Med. Biol.* **2000**, *26*, 543.
7. Koeppe, R.; Frey, K.; Synder, S.; Meyer, P.; Kilbourn, M.; Kuhl, D. *J. Cereb. Blood. Flow* **1999**, *19*, 1150.
8. Namba, H.; Iyo, M.; Shinotoh, H.; Nakatsuka, S.; Fukushi, K.; Irie, T. *Lancet* **1998**, *351*, 881.
9. Bencherif, B.; Musachio, J.; Villalobos, A.; Hilton, J.; Ravert, H.; Mathews, W.; Dannals, R.; Williams, S.; Frost, J. *J. Nucl. Med.* **1999**, *40*, 272.
10. Musachio, J.; Flesher, J.; Scheffel, U.; Rauseo, P.; Hilton, J.; Mathews, W.; Ravert, H.; Dannals, R.; Frost, J. *Nucl. Med. Biol.* **2002**, *29*, 547.
11. Irie, T.; Fukushi, K.; Akimoto, Y.; Tamagami, H.; Nozaki, T. *Nucl. Med. Biol.* **1994**, *21*, 801.
12. Kilbourn, M.; Snyder, S.; Sherman, P.; Kuhl, D. *Synapse* **1996**, *22*, 123.
13. Irie, T.; Fukushi, K.; Namba, H.; Iyo, M.; Tamagami, H.; Nakatsuka, S.; Akimoto, Y.; Ikota, N. *J. Nucl. Med.* **1996**, *37*, 649.
14. Shinotoh, H.; Namba, H.; Yamaguchi, M.; Fukushi, K.; Nagatsuka, S.; Iyo, M.; Hattori, T.; Tannada, S.; Irie, T. *Ann. Neurol.* **1999**, *46*, 62.
15. Namba, H.; Iyo, M.; Shinotoh, H.; Nagatsuka, S.; Suhara, T.; Sudo, Y.; Suzuki, K.; Irie, T. *Eur. J. Nucl. Med.* **1999**, *28*, 135.
16. Namba, H.; Irie, T.; Fukushi, K.; Iyo, M. *Brain Res.* **1994**, *667*, 278.
17. Zhang, M.-R.; Tsuchiyama, A.; Haradahira, T.; Yoshida, Y.; Irie, T.; Suzuki, K. *Nucl. Med. Biol.* **2002**, *29*, 463.
18. Krupka, M. *Biochem.* **1966**, *5*, 1988.
19. Deves, R.; Krupka, R. *Biochim. Biophys. Acta* **1979**, *557*, 469.
20. Clary, G.; Tsai, C.; Guynn, R. *Arch. Biochem. Biophys.* **1987**, *254*, 214.
21. Mulholland, G.; Mock, B.; Zheng, Q. H.; Vavrck, M. *J. Labelled Compd. Radiopharm.* **1999**, *42*, s318.
22. Jewett, D. *Appl. Radiat. Isot.* **1992**, *43*, 1383.
23. Zhang, M.-R.; Tsuchiyama, A.; Haradahira, T.; Yoshida, Y.; Irie, T.; Suzuki, K. *J. Labelled Compd. Radiopharm.* **2001**, *44* (suppl. 1), S883.
24. Zhang, M.-R.; Tsuchiyama, A.; Haradahira, T.; Yoshida, Y.; Furutsuka, T.; Suzuki, K. *Appl. Radiat. Isot.* **2002**, *57*, 335.
25. Zhang, M.-R.; Haradahira, T.; Maeda, J.; Okauchi, T.; Kawabe, K.; Kida, T.; Obayashi, S.; Suzuki, K.; Suhara, T. *Nucl. Med. Biol.* **2002**, *29*, 469.
26. Ding, Y.-S.; Fowler, J.; Dewey, S.; Wolf, A.; Logan, J.; Gatley, J.; Volkow, N.; Shea, C.; Taylor, D. *J. Nucl. Med.* **1993**, *34*, 246.
27. Okauchi, T.; Suhara, T.; Maeda, J.; Kawabe, K.; Obayashi, S.; Suzuki, K. *Synapse* **2001**, *41*, 87.